Hindawi Publishing Corporation
Mathematical Problems in Engineering
Volume 2009, Article ID 531024, 10 pages
doi:10.1155/2009/531024

Research Article

Time-Dependent Circular Billiard

J. E. Howard

Center for Integrated Plasma Studies, Laboratory for Atmospheric and Space Physics, University of Colorado, Boulder, CO 80309, USA

Correspondence should be addressed to J. E. Howard, jhoward@colorado.edu

Received 6 May 2009; Revised 8 July 2009; Accepted 15 July 2009

Recommended by Edson Denis Leonel

We investigate a time-dependent circular billiard with a two-frequency driving function and derive a new simplified form for the map, which is a symplectic nontwist map. Stability boundaries and reconnection thresholds are derived for fixed points and period-two vortex pairs. An island interspersal condition is derived such that neighboring island chains of the first frequency are exactly separated by those of the second. The results show a strong enhancement of the KAM barrier to chaotic diffusion with increasing second frequency content and overall amplitude.

1. Introduction

There is much current interest in the construction of billiard maps for systems with moving walls. For an introduction to the physics of particle confinement with moving walls, see Loskutov et al. [1]. For single frequency motion, it is well known that Fermi acceleration does not occur in the Fermi map with smooth wall motion, but does occur for a sawtooth profile [2]. In the case of the circular billiard Kamphorst and de Carvalho [3] (KdC) have proven that if the wall motion $R(t)$ is T-periodic and C^7 then Fermi acceleration does not occur, which suggests a need for numerical experiments. Two-frequency techniques were first used as a means of enhancing plasma wave heating [4]. Indeed, the two-frequency Fermi map was studied as a simplified model for plasma wave heating [4]. Each frequency carries its own series of resonances, and parameters are chosen such that the resonant islands are interspersed at a desired location. For a nearly integrable system each island chain possesses a surrounding chaotic layer, and it is these layers that "overlap", destroying local invariant circles and thereby enhancing local chaoticity. Later on, similar techniques were applied to the important physical problem of microwave ionization of Rydberg atoms [5]. Here the system is 3/2 degrees of freedom and one must make several canonical transformations in order to identify local wave-particle resonances. An experiment was designed and successfully run [6, 7], which verified a predicted enhancement in the ionization curve.

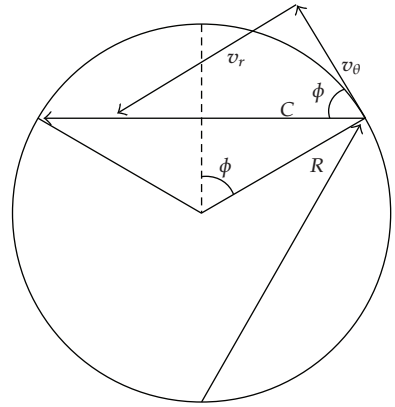

Figure 1: Geometry of the circular billiard map.

For billiards the motivating question is the existence or nonexistence of Fermi acceleration, that is, unbounded energy gain. KdC [3] showed that, based on an unpublished theorem of Douady [8], space-spanning invariant circles exist in a 2D map for harmonic oscillations of a circular billiard. On the other hand it has recently been shown that the four-dimensional time-dependent elliptic billiard exhibits Fermi accleration [9]. Here we modulate a simplified version of the 2D KdC map with a second frequency in such a way that the total energy of the two components is preserved, a direct generalization of earlier work [10]. An island interspersal condition is derived such that the second frequencies' islands fall exactly halfway in-between those of the first. The results show significant raising of the KAM barrier to global diffusion with increasing harmonic content. An important difference from previous examples is the presence of nontwist islands [11], which occur in pairs and can complicate the island overlap criterion.

2. The Circular Billiard Map

Following KdC we consider a breathing billiard of radius $R = R_0(1 + A\sin(2\pi t))$, where A is the oscillation amplitude. In the spirit of the classical Fermi map [2] we fix $R = R_0$ and ignore multiple collisions with the wall. For specular collisions the angular momentum is conserved and we map (v_r, t) from collision to collision. Figure 1 illustrates the geometry, where the angular momentum v_θ is preserved. As in [10], we neglect variations in R (which we fix at unity) but retain $V(t) = \dot{R}$ to obtain

$$T : \begin{cases} v_r' = v_r - 2V(t), \\ t' = t + \dfrac{2v_r'}{v_r'^2 + v_\theta^2} \quad (\mathrm{mod}1), \end{cases} \tag{2.1}$$

where v_r is the particle's radial velocity and $V(t)$ is the specified wall velocity. It has generating function

$$F_2(t', v_r) = t'v_r - \ln\left(v_r^2 + v_\theta^2\right) - 2\int^{t'} V(t')dt' \tag{2.2}$$

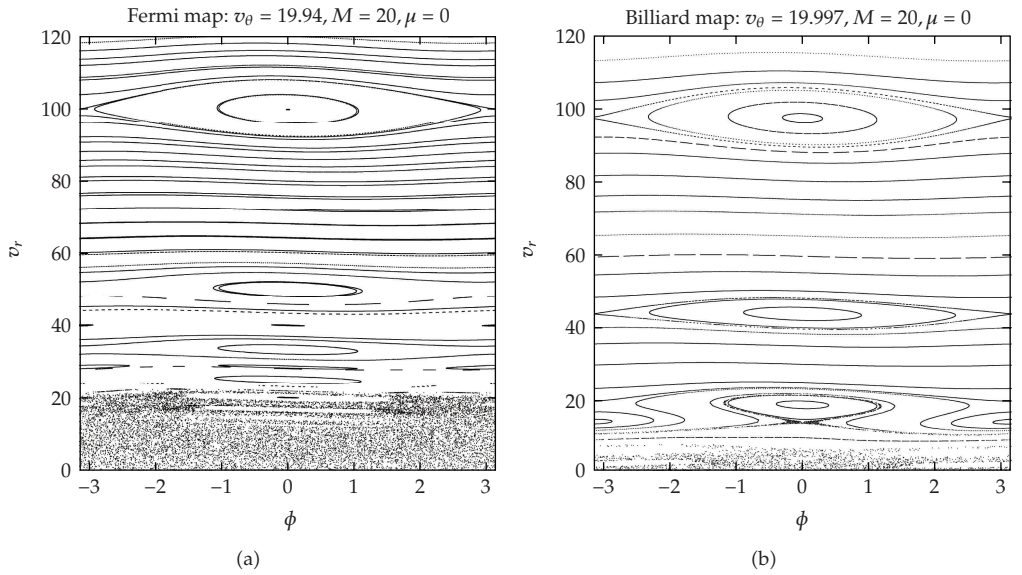

Figure 2: Comparison of circular billiard map with Fermi map for $M = 2$ and (a) $v_\theta = 19.94$ and (b) $v_\theta = 19.997$. The island centers have been shifted to $\phi = 0$.

and is therefore symplectic. The first equation follows from Figure 1, from which the half-chord $C = (1/2)v'\Delta t = R\sin\phi = Rv_r/v'$, where ϕ is the angle between v and v_θ. It has unit Jacobian and when $v_\theta \mapsto 0$, reduces to the area preserving Fermi map. The factors of two arise from the fact that there is no "there and back" for the billiard map. The same map can also be obtained by setting R = constant in KdC's somewhat more complex version. It agrees well with KdC's full map.

Before analyzing this map we first transform it so that direct comparison with the Fermi map is possible. First let $V(t) = V_0\sin(\omega t)$ and introduce the phase $\phi = \omega t$. Then, with $v_r \to 2V_0 v_r, v_\theta \to 2V_0 v_\theta$ and taking $M = \omega/2\pi V_0$ gives

$$T_2 : \begin{cases} v_r' = v_r - \sin\phi, \\ \phi' = \phi + (2\pi M)\dfrac{v_r'}{v_r'^2 + v_\theta^2} \quad (\mathrm{mod}\, 2\pi). \end{cases} \tag{2.3}$$

In the limit as $v_\theta \to 0$ we recover the Fermi map [2], for which $\phi' = \phi + 2\pi M/v_r$. Figure 2 compares the map T_2 with the Fermi map. For $v_\theta = 0$ the maps are identical but for $v_\theta = 16.5$ nontwist features appear at the bottom of the billiard map.

2.1. Stability of Fixed Points

The fixed points are given by $\phi = (0, \pi)$ and

$$\frac{Mv_r}{v_r^2 + v_\theta^2} = k \tag{2.4}$$

which occur in pairs

$$v_r^{\pm} = \frac{1}{2}\left(\frac{M}{k} \pm \sqrt{\left(\frac{M}{k}\right)^2 - 4{v_\theta}^2}\right). \tag{2.5}$$

They are linearly stable for $|\tau| = |\mathrm{Tr}\,\mathcal{J}| < 2$, where $\mathcal{J}$ is the Jacobian matrix of the map [2, 12]. We find, for $k = 1$,

$$0 < 2\pi M \cos\phi \frac{v_\theta^2 - v_r^2}{\left(v_r^2 + v_\theta^2\right)^2} < 1. \tag{2.6}$$

With the help of the equilibrium condition (2.4) this yields the stability boundaries.

Saddle-Node Bifurcation ($\tau = 2$)

We have either $v_r = 0$ or

$$v_r = v_\theta = \frac{M}{2}. \tag{2.7}$$

Period-Doubling Bifurcation ($\tau = -2$)

There is

$$\frac{\pi}{2M}\cos\phi\left(v_\theta^2 - v_r^2\right) = v_r^2. \tag{2.8}$$

For $\phi = 0$ we find either $v_r = 0$ or

$$\begin{aligned} v_r &= \frac{M\pi}{2(\pi + M)}, \\ v_\theta &= v_r\sqrt{\frac{\pi + 2M}{\pi}}, \end{aligned} \tag{2.9}$$

and for $\phi = \pi$, either $v_r = 0$ or

$$\begin{aligned} v_r &= \frac{M\pi}{2(\pi - M)}, \\ v_\theta &= v_r\sqrt{\frac{\pi - 2M}{\pi}}. \end{aligned} \tag{2.10}$$

Note that the second case is unlikely to occur, since it requires $M < (1/2)\pi$.

2.2. Reconnection

Reconnection is a global bifurcation wherein fixed points do not change type, but the separatrix layers surrounding them undergo a topological rearrangement [11]. As the effect is generic and described in detail elsewhere [11], we will be succinct. Near a resonance we have the approximate Hamiltonian [2]

$$\begin{aligned} H(t, v_r, n) &= \pi M \ln\left(v_r^2 + v_\theta^2\right) + \cos\phi\delta_1(n) \\ &\approx \pi M \ln\left(v_r^2 + v_\theta^2\right) - 2\pi v_r + \cos\phi, \end{aligned} \tag{2.11}$$

where $\delta_1(n) = \sum_{m=-\infty}^{\infty} \delta(n-m)$. In deriving (2.11) we Fourier analyzed $\delta_1(n)$ and averaged over higher-order resonances. We also Taylor expanded H in the vertical direction.

The reconnection threshold is given by equating the value of $\overline{H}$ on neighboring separatrices. With this definition, we calculate $\overline{H}_{\text{lower}} = 1$ and

$$\overline{H}_{\text{upper}} = \pi M_e \ln\left(\frac{(v_r^+)^2 + {v_\theta}^2}{(v_r^-)^2 + v_\theta^2}\right) - 2\pi\left(v_r^+ - v_r^-\right) - 1, \tag{2.12}$$

where $v_r^\pm = (1/2)(M_e \pm \sqrt{M_e^2 - 4v_\theta^2})$. Equating $H_{\text{upper}} = H_{\text{lower}}$ then gives

$$\frac{1}{\pi M_e} = \ln\left(\frac{1+\sqrt{1-\tilde{v}^2}}{\tilde{v}}\right) - \sqrt{1-\tilde{v}^2}, \tag{2.13}$$

where $\tilde{v} = 2v_\theta/M_e$. Figure 3 shows a typical reconnection with $M = 20$. Equation (2.14) shows that this occurs for $v_\theta = 9.355$, in excellent agreement with the figure. Essentially perfect agreement occurs for larger M, where the chaotic layer is thinner.

2.3. Vortex Pairs

Vortex pairs also exist for this map. Figure 4 shows such a pair for $M = 20$ and $v_\theta = 19.94$ and 19.997. To understand this structure, consider a general period-two orbit, for which $\sin\phi + \sin\phi' = 0$, so that either $\phi' = -\phi$ or $\phi' = \phi - \pi$. The former orbits do not exist for all parameters, being born in a pitchfork bifurcation. The latter orbits turn out to have $\phi = \pi$, $\phi' = 0$, with $2Mv_r/(v_r^2+v_\theta^2) = 1$. They are stable for $\pi M_e|f'(v_r)| < 1$, where $f(v_r) = v_r/(v_r^2+v_\theta^2)$. It follows that $v_r = v_r'$ and $v_r^2 - 2Mv_r + v_\theta^2 = 0$, so that

$$v_r = M \pm \sqrt{M^2 - v_\theta^2}. \tag{2.14}$$

Thus, vortex pairs annihilate when $v_\theta = M$, in agreement with Figure 4. They are formed when x-points of adjacent island chains merge. Note that vortex pair configuration is extremely ephemeral and therefore probably of little importance in particle transport. For details see [11].

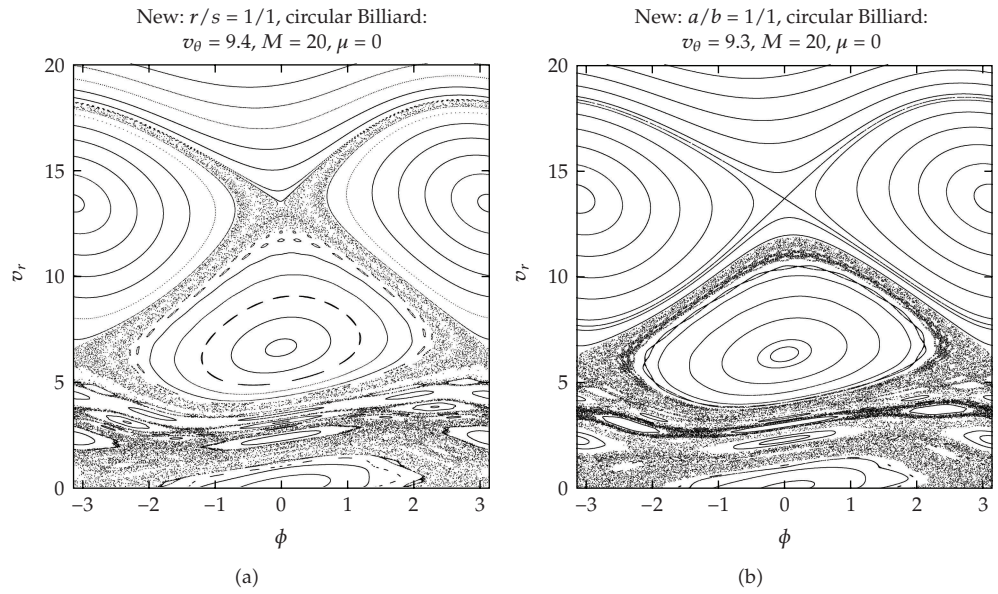

Figure 3: Circular Billiard map for $M = 20$ and (a) $v_\theta = 9.4$, (b) $v_\theta = 9.3$, illustrating reconnection.

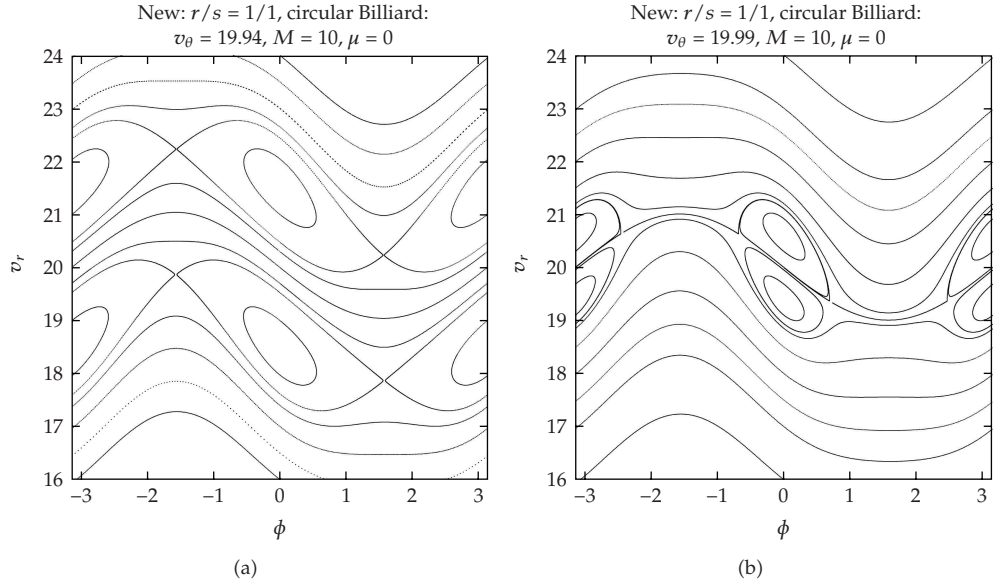

Figure 4: Vortex pair formation for circular billiard map for $M = 20$ and (a) $v_\theta = 19.99$, (b) $v_\theta = 19.997$.

3. A Two-Frequency Map

Following the program of [10] we employ the bichromatic wall function

$$V(\phi) = \frac{V_a \sin(\omega_a t) + V_b \sin(\omega_b t)}{\sqrt{V_a^2 + V_b^2}}, \tag{3.1}$$

where V_a and V_b are the amplitudes, and ω_a and ω_b are the frequencies of the two components. The condition

$$V_a^2 + V_b^2 = \text{const} \tag{3.2}$$

maintains constant energy in the two waves, while the frequencies are chosen such that

$$\frac{\omega_a}{\omega_b} = \frac{a}{b} \tag{3.3}$$

where a and b are coprime integers, in order to maintain periodicity.

Defining the phase $\phi = \omega_a t/a$, the map T_2 can be written

$$T_3 : \begin{cases} v_r' = v_r - V(\phi), \\ \phi' = \phi + \left(\dfrac{4\pi M}{a+b}\right)\dfrac{v_r'}{v_r'^2 + v_\theta^2} \pmod{2\pi}, \end{cases} \tag{3.4}$$

where $M = \overline{\omega}/\pi$ and

$$\frac{\omega_a}{a} = \frac{\omega_b}{b} = \frac{\overline{\omega}}{a+b} \tag{3.5}$$

with $\overline{\omega} = (1/2)(\omega_a + \omega_b)$. Thus (3.1) becomes

$$V(\phi) = \frac{\left[\sin(a\phi) + \mu \sin(b\phi)\right]}{\sqrt{1+\mu^2}}, \tag{3.6}$$

where $\mu = V_b/V_a$.

3.1. Island Interspersal

For the map T_3 we may distinguish three distinct families: *common* resonances, which are shared by both a-and b-fold frequencies and defined by $\phi \mapsto \phi + 2\pi k$,

$$\frac{v_r}{v_r^2 + v_\theta^2} = \frac{k}{M_e} \tag{3.7}$$

with effective $M_e = 2M/(a+b)$ or

$$v_r^2 - \frac{M_e}{k} v_r + v_\theta^2 = 0 \tag{3.8}$$

with solution

$$v_{rk}^{\pm} = \frac{1}{2}\left(\frac{M_e}{k} \pm \sqrt{\left(\frac{M_e}{k}\right)^2 - 4v_\theta^2}\right). \tag{3.9}$$

The angle ϕ_0 is given by

$$\sin a\phi + \mu \sin b\phi = 0. \tag{3.10}$$

In addition, when $\mu = 0$ there exists a set of fixed points given by $a\phi \mapsto a\phi + 2\pi k$, which includes the common set (3.7):

$$\frac{av_{rk}}{v_{rk}^2 + v_\theta^2} = \frac{k}{M_e}. \tag{3.11}$$

These fixed points have period P, where P/Q is a/b reduced to the lowest terms. Similarly, when $\mu \mapsto \infty$, setting $b\phi \mapsto b\phi + 2\pi k$ yields period-b fixed points, given by

$$\frac{bv_{rk}}{v_{rk}^2 + v_\theta^2} = \frac{k}{M_e}, \tag{3.12}$$

which also includes (3.7) as a subset. At intermediate values of μ the a- and b-fold islands at $\phi_0 = 0$ and π are unperturbed, while the other fixed points move according to (3.10), which locates $\phi_0(\mu)$.

Figure 5 compares the two-frequency Billiard map for $a = 3$, $b = 2$, $v_\theta = 16$ for $\mu = 0.0$ and $\mu = 0.25$. The general effect follows closely that for the Fermi map [10]. For $\mu = 0.25$ one can see the groups of three a-fold islands interspersed with groups of two b-fold islands. One can also see chains of five islands, due to nonlinear mixing of the 2 and 3-fold chains. Increasing the admixture μ causes the amplitude of the b-fold islands to increase to the point where two neighboring a-chains "overlap." The net effect is to raise the KAM barrier; maximal chaos is attained for $\mu \approx 0.5$. Figure 6 shows the result of iterating a single orbit with intial condition $\phi = 0$, $v_r = 10$. For $\mu = 0.0$ the orbit hangs up on the twistless torus near $v_r = 20$, but for $\mu = 0.5$ it breaks through and reaches a new KAM barrier near $v_r = 70$. Interesting complications can arise due to pairs of islands and their bifurcations. Using the "two-thirds rule," one can be quite quantitative about overlap, [10] but that is not our present goal, which is to demonstrate that the KAM barrier can indeed be raised substantially.

4. Discussion

We have derived a simplified version of the circular billiard map, which promises to be very useful in parametric studies. As an example we have studied the effects of two frequencies and demonstrated the raising of the KAM barrier to diffusion. The map can be "straightened"

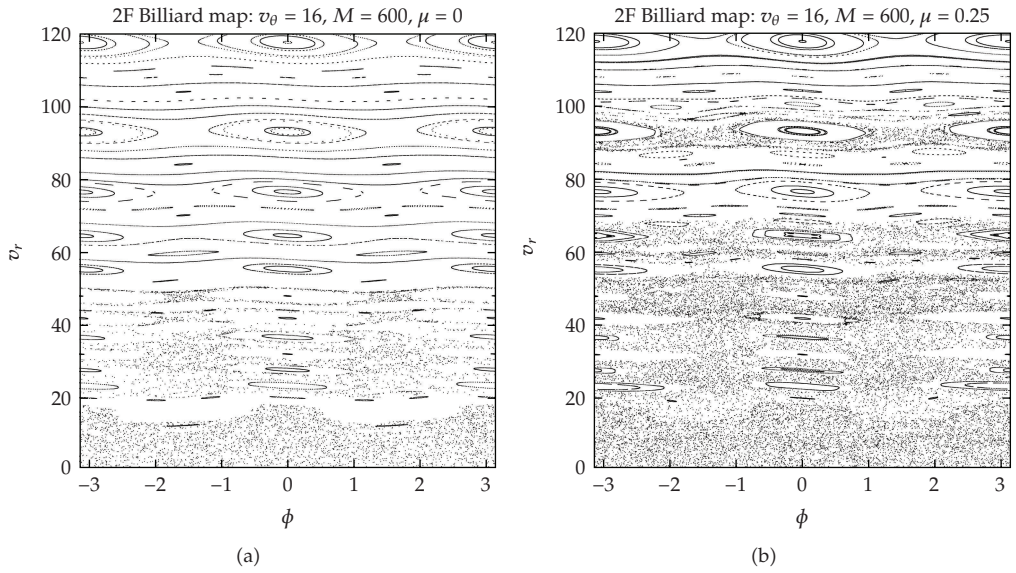

Figure 5: A Two-frequency Fermi map for $M = 600,\ a = 3,\ b = 2,\ v_\theta = 16$ for (a) $\mu = 0.0$, (b) $\mu = 0.25$.

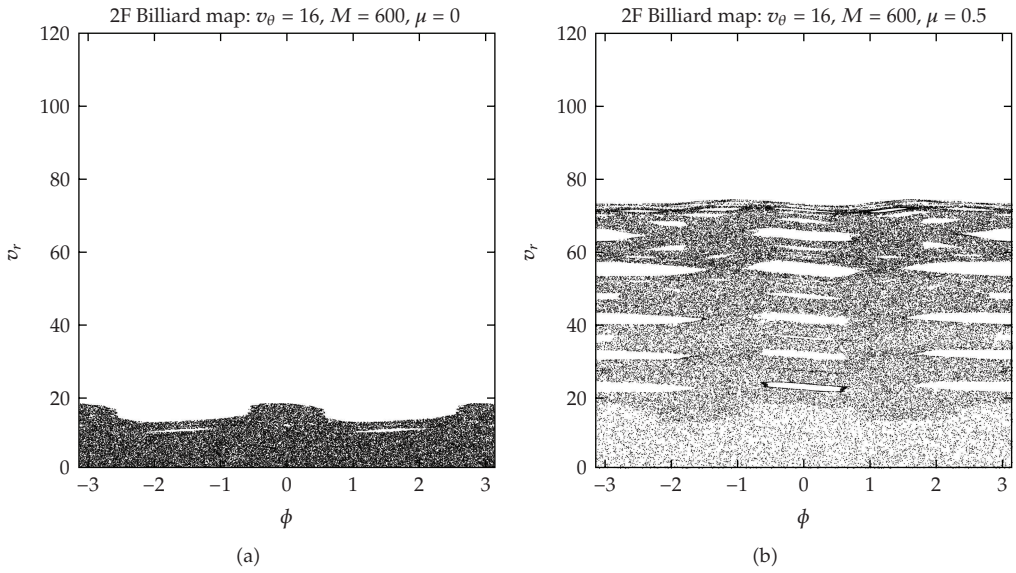

Figure 6: Single orbits; 10^6 iterations for $M = 600,\ a = 3,\ b = 2,\ v_\theta = 16$ (a) with $\mu = 0$, (b) $\mu = 0.5$.

by adding appropriate terms to the map. It was surprising to encounter a nontwist map and one wonders how this fact would manifest itself in the 4D elliptic billiard. We emphasize that the chaos enhancement effect of using two frequencies is *not* Fermi acceleration; the motion is still firmly bounded by the existence of space-spanning invariant circles.

Acknowledgments

It is a pleasure to acknowledge the contributions of Professor J. D. Meiss, A. Loskutov, S. M. Soskin and S. Kamphorst. A preliminary version of this paper was given at the Conference Billiards09, in Aquas de Lindóia, Brazil. The author is grateful to Professor E. Leonel for inviting him to this conference.

References

[1] A. Loskutov, A. B. Ryabov, and L. G. Akinshin, "Properties of some chaotic billiards with time-dependent boundaries," *Journal of Physics A*, vol. 33, no. 44, pp. 7973–7986, 2000.

[2] A. J. Lichtenberg and M. L. Lieberman, *Regular and Chaotic Dynamics*, Springer, New York, NY, USA, 1980.

[3] S. O. Kamphorst and S. P. de Carvalho, "Bounded gain of energy on the breathing circle billiard," *Nonlinearity*, vol. 12, no. 5, pp. 1363–1371, 1999.

[4] J. E. Howard, A. J. Lichtenberg, M. A. Lieberman, and R. H. Cohen, "Four-dimensional mapping model for two-frequency electron cyclotron resonance heating," *Physica D*, vol. 20, no. 2-3, pp. 259–284, 1986.

[5] J. E. Howard, "Theory of two-frequency microwave ionization of hydrogen atoms," *Physics Letters A*, vol. 156, no. 6, pp. 286–292, 1991.

[6] A. Haffmans, R. Blümel, P. M. Koch, and L. Sirko, "Prediction of a new peak in two-frequency microwave "ionization" of excited hydrogen atoms," *Physical Review Letters*, vol. 73, no. 2, pp. 248–251, 1994.

[7] L. Sirko, S. Yoakum, A. Haffmans, and P. M. Koch, "Microwave-driven He Rydberg atoms: Floquet-state degeneracy lifted by a second frequency, Stueckelberg oscillations, and their destruction by added noise," *Physical Review A*, vol. 47, no. 2, pp. R782–R785, 1993.

[8] R. Douady, "These de 3eme cycle (unpublished)," Universite Paris VII, 1982.

[9] F. Lenz, F. K. Diakonos, and P. Schmelcher, "Tunable fermi acceleration in the driven elliptical billiard," *Physical Review Letters*, vol. 100, no. 1, Article ID 014013, 2008.

[10] J. E. Howard, A. J. Lichtenberg, and M. A. Lieberman, "Two-frequency Fermi mapping," *Physica D*, vol. 5, no. 2-3, pp. 243–257, 1982.

[11] J. E. Howard and S. M. Hohs, "Stochasticity and reconnection in Hamiltonian systems," *Physical Review A*, vol. 29, no. 1, pp. 418–421, 1984.

[12] J. E. Howard and R. S. MacKay, "Linear stability of symplectic maps," *Journal of Mathematical Physics*, vol. 28, no. 5, pp. 1036–1051, 1987.